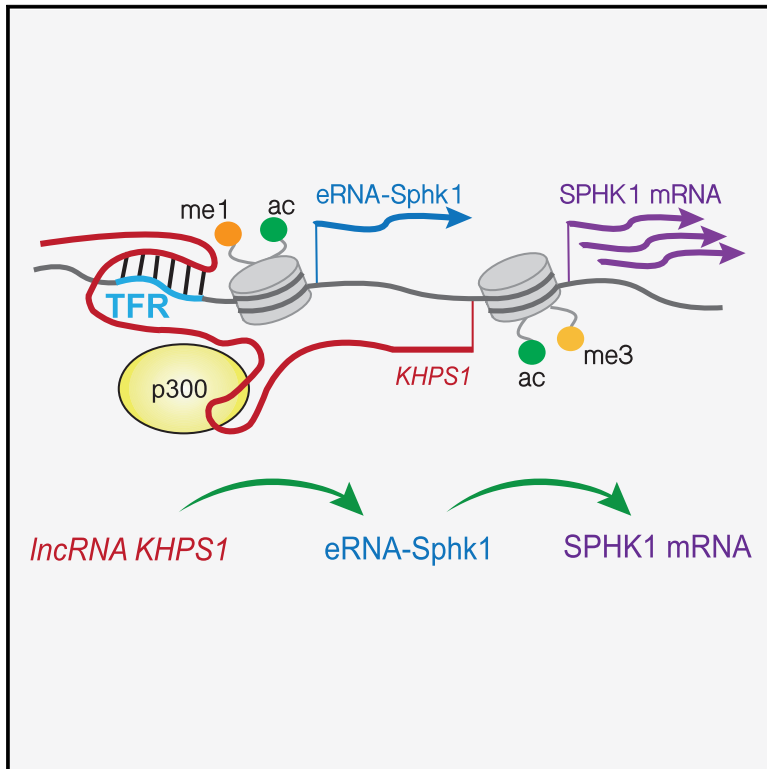


## lncRNA *KHPS1* Activates a Poised Enhancer by Triplex-Dependent Recruitment of Epigenomic Regulators

### Graphical Abstract



### Authors

Alena Blank-Giwojna,  
Anna Postepska-Igielska, Ingrid Grummt

### Correspondence

i.grummt@dkfz-heidelberg.de

### In Brief

Blank-Giwojna et al. demonstrate that the antisense RNA *KHPS1* forms an RNA-DNA triplex at the *SPHK1* enhancer. Tethering *KHPS1* to the enhancer is required for recruitment of E2F1 and p300, transcription of enhancer-derived RNA, and activation of *SPHK1* expression. The results uncover a triplex-driven feedforward mechanism of transcriptional regulation.

### Highlights

- RNA-DNA triplex formation is required for transcription activation of the proto-oncogene *SPHK1*
- lncRNA bound to the *SPHK1* induces the synthesis of eRNA-Sphk1 and *SPHK1* mRNA
- eRNA-Sphk1 evicts CTFC, which insulates the enhancer from the *SPHK1* promoter
- Deletion of the triplex-forming region impairs *SPHK1* expression and cell viability



# lncRNA *KHPS1* Activates a Poised Enhancer by Triplex-Dependent Recruitment of Epigenomic Regulators

Alena Blank-Giwojna,<sup>1</sup> Anna Postepska-Igielska,<sup>1</sup> and Ingrid Grummt<sup>1,2,\*</sup>

<sup>1</sup>Molecular Biology of the Cell II, German Cancer Research Center (DKFZ), DKFZ-ZMBH Alliance, 69120 Heidelberg, Germany

<sup>2</sup>Lead Contact

\*Correspondence: [i.grummt@dkfz-heidelberg.de](mailto:i.grummt@dkfz-heidelberg.de)

<https://doi.org/10.1016/j.celrep.2019.02.059>

## SUMMARY

Transcription of the proto-oncogene *SPHK1* is regulated by *KHPS1*, an antisense RNA that activates *SPHK1* expression by forming a triple-helical RNA-DNA-DNA structure at the *SPHK1* enhancer. Triplex-mediated tethering of *KHPS1* to its target gene is required for recruitment of E2F1 and p300 and transcription of the RNA derived from the *SPHK1* enhancer (eRNA-Sphk1). eRNA-Sphk1 evicts CTCF, which insulates the enhancer from the *SPHK1* promoter, thus facilitating *SPHK1* expression. Genomic deletion of the triplex-forming sequence attenuates *SPHK1* expression, leading to decreased cell migration and invasion. Replacement of the triplex-forming region (TFR) of *KHPS1* by the TFR of the lncRNA *MEG3* tethers *KHPS1* to the *MEG3* target gene *TGFBR1*, underscoring the interchangeability and anchoring function of sequences involved in triplex formation. Altogether, the results reveal a triplex-driven feedforward mechanism involving lncRNA-dependent induction of eRNA, which enhances expression of specific target genes.

## INTRODUCTION

Antisense transcription is increasingly recognized as an important regulator of gene expression, acting as a modular scaffold for protein complexes that can rewire regulatory networks. The genomic arrangement of antisense RNA genes suggests that they might be a part of circuits that allow genes to regulate their own expression. The intrinsic flexibility of RNA molecules supports that antisense transcripts, and long noncoding RNAs (lncRNAs) in general, act as molecular platforms in which different domains associate with DNA, RNA, or proteins. By interacting with multiple proteins, lncRNAs enable recruitment of chromatin-modifying enzymes and transcription regulators that control the chromatin state and activity of specific genes (Long et al., 2017; Chen et al., 2018). A distinct class of noncoding RNAs (ncRNAs), known as enhancer-derived RNAs (eRNAs), activates transcription of specific target genes by stabilization

of enhancer-promoter interactions (De Santa et al., 2010; Kim et al., 2010; Ørom et al., 2010).

A wealth of transcriptomics data has demonstrated the presence and functional relevance of numerous lncRNAs. However, it remains elusive how they function at the molecular level and how they are targeted to specific genomic sites. Because RNA has the ability to recognize and bind specific DNA sequences, it can hybridize with single-stranded DNA, forming RNA-DNA duplexes known as R loops (Thomas et al., 1976), or directly bind to the major groove of purine-rich double-stranded DNA via Hoogsteen base pairing, forming RNA-DNA-DNA triplex structures (Felsenfeld et al., 1957; Li et al., 2016). *In silico* analyses have identified numerous lncRNAs with triplex-forming domains, which may engage in triplex structures with respective purine-rich DNA sequences (Goñi et al., 2004; Buske et al., 2012; Soibam, 2017). Such specific structures may mark the genome and dictate how lncRNA-associated transcription regulators and chromatin-modifying enzymes are guided to appropriate genomic sequences. Significantly, sequences with triplex-forming potential are overrepresented at regulatory gene regions, such as promoters and enhancers, suggesting that RNA-DNA triplex formation may represent a general mechanism for lncRNA-mediated recognition of target sites in the genome.

Examples for lncRNAs that associate with specific DNA sequences via triplex formation include promoter-associated RNA (pRNA), which silences transcription of rRNA genes by targeting DNMT3b to the rDNA promoter (Schmitz et al., 2010); PAPAS, an lncRNA that is transcribed in antisense orientation to pre-rRNA and facilitates recruitment of the CHD4/NuRD repressor to rDNA (Zhao et al., 2018); *Fendrr*, which facilitates tissue differentiation by targeting the PRC2 complex to developmental genes (Grote et al., 2013); and *MEG3*, which guides PRC2 to transforming growth factor  $\beta$  (TGF- $\beta$ )-responsive genes (Mondal et al., 2015). Furthermore, *PARTICLE* and *HOTAIR*, as well as some microRNAs (miRNAs), were shown to regulate expression of specific target genes and to directly interact with DNA (O'Leary et al., 2015; Kalwa et al., 2016; Paugh et al., 2016). Another example is *KHPS1*, an RNA that is synthesized in antisense orientation to the proto-oncogene *SPHK1* (sphingosine kinase 1) and is required for activation of *SPHK1* transcription (Imamura et al., 2004; Postepska-Igielska et al., 2015). Transcription of *KHPS1* is associated with recruitment of *KHPS1*-associated transcriptional co-activators to *SPHK1* that establish a transcription-permissive chromatin structure (Postepska-Igielska et al., 2015).



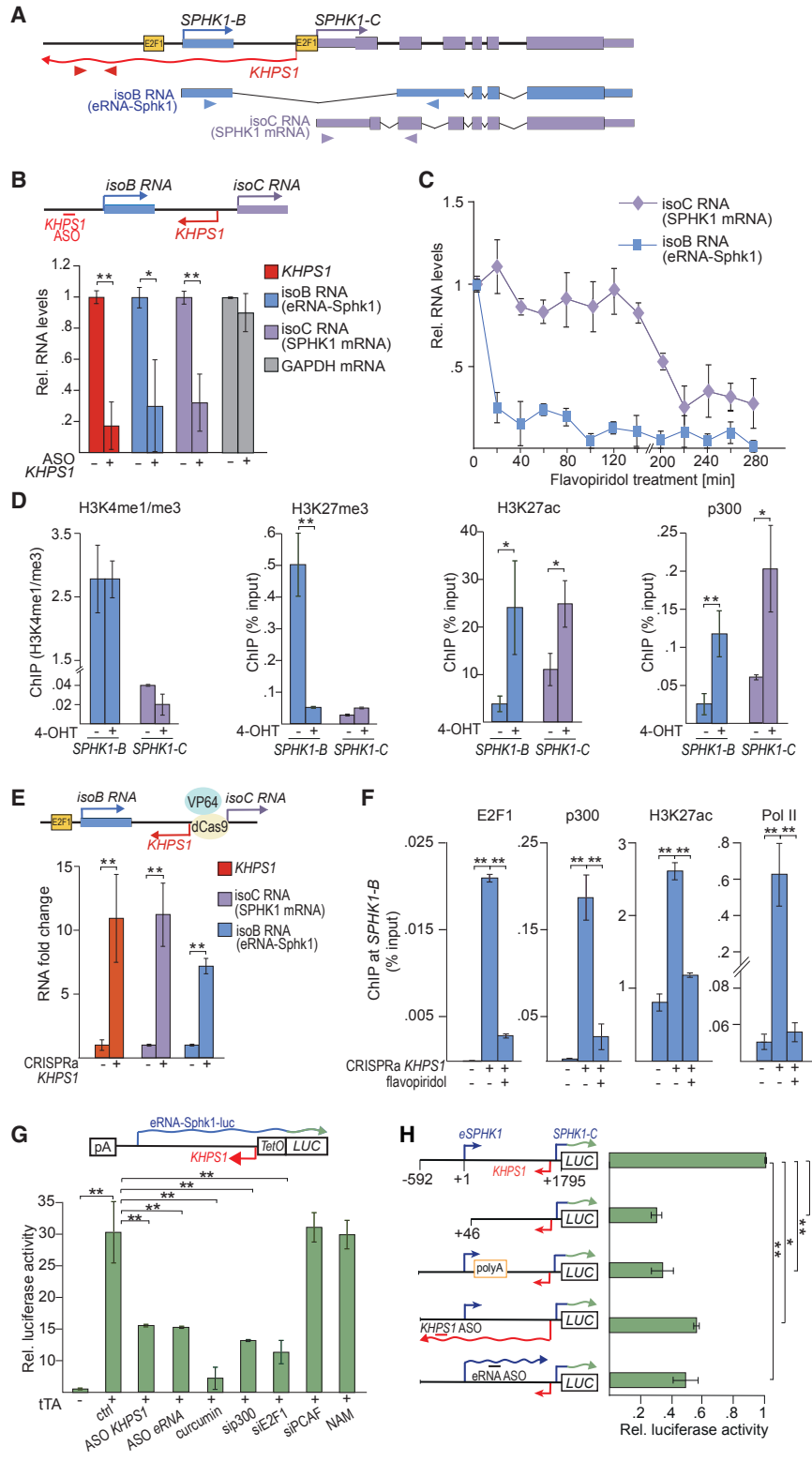


**Figure 1. lncRNA KHPS1 Activates a Poised Enhancer**

(A) Scheme of the human *SPHK1* locus. Exons of *SPHK1-B* and *SPHK1-C* are presented as blue and purple boxes, respectively; black lines represent introns. The transcription start sites of *KHPS1*, isoB RNA (eRNA-Sphk1), and *SPHK1* mRNA (isoC RNA) are marked by arrows. E2F1 binding sites are boxed. The positions of primers used in qPCR to monitor the levels of *KHPS1*, eRNA-Sphk1, and *SPHK1* mRNA are indicated by colored arrowheads.

(legend continued on next page)

However, none of the previous studies, including ours, provided rigorous proof that RNA-DNA triplex structures are physiologically relevant. Here we provide compelling experimental evidence for triplex-dependent regulation of gene expression. We show that binding of *KHPS1* to a triplex-forming region upstream of the *SPHK1* promoter is indispensable for activation of a poised enhancer. The activated enhancer produces eRNA, which is required for SPHK1 expression and cell proliferation. Transcription of messenger RNA encoding SPHK1 (SPHK1 mRNA) depends on binding of *KHPS1* to a purine-rich sequence at the enhancer, forming a triple helical RNA-DNA structure. Tethering *KHPS1* to DNA guides associated regulatory proteins to the *SPHK1* enhancer and facilitates transcription of the RNA derived from the *SPHK1* enhancer (eRNA-Sphk1). Genomic deletion of the triplex-forming region (TFR) or prevention of *KHPS1* binding to DNA by ectopic TFR-containing RNA impairs cell proliferation and viability. Significantly, replacement of the *KHPS1* TFR by the TFR of the lncRNA *MEG3* targets *KHPS1* to the *MEG3* target gene *TGFBR1*. The results demonstrate the functional relevance of RNA-DNA triplexes and decipher a regulatory feedforward mechanism that depends on triplex-mediated guidance of lncRNA-associated regulatory proteins to distinct genomic loci.

## RESULTS

### *KHPS1* Activates a Poised Enhancer

The human *SPHK1* locus comprises different gene isoforms, with transcription from the *SPHK1-C* (isoform C [isoC]) promoter giving rise to alternatively spliced mRNAs that encode three isoforms of the SPHK1 protein (Figures 1A and S1A) (Paugh et al., 2009). Transcription from the E2F1-regulated *SPHK1-C* promoter also directs the synthesis of a long antisense transcript, termed *KHPS1* (Imamura et al., 2004; Postepska-Igielska et al., 2015), indicating that *SPHK1-C* is a bidirectional promoter that governs transcription of SPHK1 mRNA in the sense direction and *KHPS1* in the antisense orientation. Significantly, transcription of *KHPS1* is required for activation of the *SPHK1-B* promoter (Postepska-Igielska et al., 2015). Knockdown of *KHPS1* by antisense oligonucleotides (ASOs) led to decreased levels of both

isoB and isoC RNAs, indicating that *KHPS1* regulates transcription of sense RNAs that originate from the *SPHK1-B* and *SPHK1-C* promoters, respectively (Figures 1B and S1B).

isoC transcripts (SPHK1 mRNA) are usually two orders of magnitude more abundant than isoB transcripts (Figure S1C). Moreover, a large fraction of isoB RNA resides in the nucleus, whereas isoC RNA is enriched in the cytoplasm (Figure S1D). To examine whether the different abundances of isoform-specific RNAs is due to different transcript stability, we determined the turnover of isoB and isoC RNAs after blocking transcription elongation with flavopiridol. Both transcripts displayed marked differences in their half-lives, with 50% of isoB RNA being degraded after 15 min, whereas isoC transcripts exhibit a half-life of about 3.5 h (Figure 1C). The different features of isoB and isoC RNAs suggest that these are distinct RNAs with diverse functions.

The nuclear localization and rapid decay of isoB RNA are reminiscent of eRNAs, which are transcribed from uni- or bidirectional promoters and regulate transcription of enhancer-associated genes (Kim et al., 2010; Li et al., 2013; Hsieh et al., 2014; Lam et al., 2014). We therefore reasoned that isoB RNA might exert the function of an eRNA that is activated by *KHPS1* and enhances isoC transcription. Inspection of available datasets revealed the presence of typical enhancer marks upstream of the transcription start site (TSS) of *SPHK1-B*, that is, enrichment of histone H3 monomethylated at lysine 4 (H3K4me1) and histone H3 acetylated at lysine 27 (H3K27ac), suggesting that *SPHK1-B* may function as a distal regulatory element (Figure S1E).

This view is supported by chromatin immunoprecipitation (ChIP) experiments using U2OS/ER-E2F1 cells that express estrogen receptor (ER)-tagged E2F1. In uninduced U2OS/ER-E2F1 cells, the *SPHK1-B* promoter displays a high H3K4me1/H3K4me3 ratio (>2), a characteristic of enhancers. However, the *SPHK1-C* promoter exhibits a low H3K4me1/H3K4me3 ratio (0.04), which marks active promoters (Figures 1D and S1F). Upon *KHPS1* induction by 4-hydroxytamoxifen (4-OHT), the increased occupancy of p300 and H3K27ac at the *SPHK1-B* promoter coincided with loss of histone H3 trimethylated at lysine 27 (H3K27me3) (Figure 1D). The increase in H3K27ac at the expense of H3K27me3, the high ratio of H3K4me1/H3K4me3, and the *KHPS1*-dependent activation of isoB

(B) qRT-PCR monitoring levels of *KHPS1*, isoB RNA (eRNA-Sphk1), isoC RNA (SPHK1 mRNA), and GAPDH mRNA in U2OS/ER-E2F1 cells transfected with control ASO (–) or *KHPS1*-specific ASO targeting nucleotides –101/–121 relative to the TSS of *SPHK1-B* (+) (N = 3).

(C) Different half-lives of isoB (eRNA-Sphk1) and isoC (SPHK1 mRNA) transcripts in U2OS/ER-E2F1 cells treated with 4-OHT (5 h) followed by inhibition of transcription by treatment with flavopiridol. The levels of isoB and isoC RNAs were monitored by qRT-PCR at the indicated times (N = 3).

(D) ChIPs showing occupancy of the indicated histone marks and p300 at the *SPHK1-B* and *SPHK1-C* promoters in uninduced U2OS/ER-E2F1 cells or after treatment with 4-OHT for 8 h (N = 3).

(E) Levels of *KHPS1*, isoC (SPHK1 mRNA), and eRNA-Sphk1 in U2OS/ER-E2F1 cells expressing dCas9-VP64 targeted to the *KHPS1* promoter by sgRNAs (–5/–25 and –49/–69 relative to the TSS of *KHPS1*) (+) or co-transfected with a control sgRNA (–) (N = 3).

(F) ChIPs showing occupancy of E2F1, p300, H3K27ac, and Pol II at e*SPHK1* in untreated U2OS/ER-E2F1 cells and after CRISPRa-mediated upregulation of *KHPS1* in the absence and presence of flavopiridol treatment (1 h) (N = 3).

(G) Reporter assay monitoring *KHPS1*-dependent activation of e*SPHK1*-driven luciferase expression. U2OS/ER-E2F1 cells were co-transfected with the reporter plasmid pTet-*KHPS1*(+1,448/–592-isoB-luc) and a plasmid encoding tTA. Where indicated, cells were transfected with ASOs against *KHPS1* or eRNA-Sphk1, with siRNAs against E2F1, p300, or PCAF or treated with curcumin (30 μM) or NAM (10 mM). Activation of eRNA-Sphk1 transcription was measured by expression of luciferase (N = 3).

(H) Reporter assay measuring *SPHK1-C*-driven luciferase expression in U2OS/ER-E2F1 cells co-transfected with the indicated pREP4-luciferase plasmids and an E2F1 expression vector. Where indicated, ASOs targeting *KHPS1* or eRNA-Sphk1 were co-transfected. The luciferase signal of pREP4-SPHK1(–592/+1,795)-luc was set to 1 (N = 3).

Data are presented as mean ± SEM. \*p < 0.05, \*\*p < 0.01.

See also Figure S1.

transcription indicate that *SPHK1-B* is a poised enhancer that is activated by *KHPS1*. Thus, the *SPHK1-B* promoter will thereafter be referred to as the *SPHK1* enhancer (*eSPHK1*), isoB transcripts will be referred to as eRNA-Sphk1, and isoC transcripts will be referred to as SPHK1 mRNA.

To substantiate the requirement of *KHPS1* for activation of the *SPHK1-B* enhancer, we took advantage of the CRISPR activation (CRISPRa) approach to induce *KHPS1* transcription. As expected, targeting of dCas9-VP64 to the bidirectional *KHPS1* promoter led to upregulation of both *KHPS1* and SPHK1 mRNA. Induction of *KHPS1* by dCas9-VP64 also led to increased levels of eRNA-Sphk1 (Figure 1E) and enhanced occupancy of E2F1, p300, RNA polymerase II (Pol II), and H3K27ac at *SPHK1-B*. Transcriptional activation and association with chromatin were compromised if Pol II transcription elongation was inhibited by flavopiridol (Figures 1F and S1G). No increase in H3K27ac was observed downstream of the TSS of *KHPS1*, supporting that dCas9-VP64-mediated changes in chromatin structure did not spread into adjacent gene regions (Figure S1H). Thus, transcription of *KHPS1* rather than binding of dCas9-VP64 triggered the establishment of a transcription-permissive chromatin structure at the *eSPHK1*.

To reinforce the importance of *KHPS1*-mediated recruitment of transcriptional co-activators and induction of eRNA-Sphk1, we generated a reporter plasmid that drives *KHPS1* transcription under the control of a tetracycline-inducible promoter. Enhancer activation was monitored by expression of luciferase, which was fused in frame with eRNA-Sphk1. Upon transfection of the tetracycline transactivator (tTA), a 30- to 40-fold increase in the luciferase signal was observed. Enhanced luciferase expression was compromised by ASO-mediated knockdown of either *KHPS1* or eRNA-Sphk1, underscoring the requirement of both regulatory RNAs for luciferase expression (Figure 1G). Increased luciferase expression was also attenuated by treatment with curcumin, an inhibitor of p300/CBP activity (Marcu et al., 2006), and by small interfering RNA (siRNA)-mediated depletion of E2F1 or p300. Knockdown of the histone acetyltransferase PCAF or treatment with nicotinamide (NAM), a specific inhibitor of NAD<sup>+</sup>-dependent deacetylases, did not affect *eSPHK1*-driven luciferase expression, reinforcing that transcription of eRNA-Sphk1 requires *KHPS1*-dependent targeting of p300/CBP and E2F1 to the *eSPHK1*.

To corroborate the enhancing function of eRNA-Sphk1 on *SPHK1-C* transcription, we transfected U2OS/ER-E2F1 cells with luciferase reporter plasmids comprising or lacking sequences upstream of the TSS of *eSPHK1* and monitored *SPHK1-C*-driven luciferase activity upon E2F1 induction. Luciferase expression was significantly higher in cells transfected with the plasmid harboring *eSPHK1* sequences from -592 to +1,795 (pREP4-SPHK1(-592/+1,795)) than in cells transfected with the reporter lacking *eSPHK1* (pREP4-SPHK1(+46/+1,795)). Insertion of a polyadenylation cassette 20 bp downstream of the TSS of *eSPHK1* reduced luciferase expression, reinforcing the importance of eRNA transcription for *SPHK1-C* transcription (Figure 1H). The level of *KHPS1* remained unchanged, corroborating that attenuation of *SPHK1-C* transcription was brought about by poly(A)-dependent termination of eRNA-Sphk1 (Figure S1I). Knockdown of either *KHPS1* or

eRNA-Sphk1 led to decreased luciferase expression, underscoring the importance of *KHPS1*-dependent induction of eRNA-Sphk1 for transcription of *SPHK1* mRNA.

### eRNA-Sphk1 Stimulates Transcription of SPHK1 mRNA

To substantiate the importance of eRNA-Sphk1 for *SPHK1-C* transcription, we monitored the level of SPHK1 mRNA after ASO-mediated knockdown of eRNA-Sphk1. Consistent with the enhancing function of eRNA-Sphk1, knockdown of eRNA-Sphk1 markedly reduced the level of SPHK1 mRNA without affecting *KHPS1* (Figures 2A, S2A, and S2B). Likewise, single guide RNA (sgRNA)-mediated targeting of the dCas9-KRAB co-repressor to *eSPHK1* decreased both eRNA-Sphk1 and SPHK1 mRNA without affecting the level of *KHPS1* (Figures 2B, left, and S2C) and attenuated binding of initiating Pol II to the *SPHK1-C* promoter (Figure 2B, right). Given that efficient KRAB-mediated repression requires targeting of sgRNAs close to the TSS (Gilbert et al., 2013; Radzisheuskaya et al., 2016), this result reveals that downregulation of SPHK1 mRNA is brought about by knockdown of eRNA-Sphk1 rather than by dCas9-KRAB-mediated repression of *SPHK1-C* transcription. Reciprocally, activation of eRNA-Sphk1 transcription by dCas9-VP64 led to increased binding of Pol II to the *SPHK1-C* promoter and elevated levels of both SPHK1 mRNA and SPHK1 proteins, whereas *KHPS1* remained unchanged (Figures 2C, S2D, and S2E). Moreover, E2F1-induced activation of *SPHK1-C* was compromised upon knockdown of eRNA-Sphk1 (Figure S2F). Depletion of INTS11, a subunit of the Integrator complex that mediates transcription termination and release of mature eRNAs (Lai et al., 2015), attenuated E2F1-mediated increase of mature eRNA-Sphk1 and reduced transcription of SPHK1 mRNA (Figures 2D and S2G), reinforcing that transcripts originating from *eSPHK1* enhance expression of SPHK1.

Given that elevated levels of SPHK1 are linked to tumor development and progression (Sarkar et al., 2005; Zhu et al., 2015), we examined whether knockdown of *KHPS1* and eRNA-Sphk1 would impair the tumorigenic potential of cells. To this end, we transfected ASOs against *KHPS1* or eRNA-Sphk1 into MDA-MB-231 cells, a breast cancer cell line that expresses high levels of SPHK1 (Datta et al., 2014). We observed a profound delay in gap closure after depletion of either *KHPS1* or eRNA-Sphk1, which was similar to the phenotype observed in cells treated with the SPHK1 inhibitor SKI II (French et al., 2003) (Figures 2E and S2H). The invasive capacity of control and ASO-treated MDA-MB-231 cells was also severely impaired after depletion of *KHPS1* or eRNA-Sphk1 (Figures 2F, S2I, and S2J). Furthermore, knockdown of either *KHPS1* or eRNA-Sphk1 prevented colony formation in soft agar, an indicator of cancer cell tumorigenicity (Figure S2K). These results demonstrate that downregulation of *KHPS1* or eRNA-Sphk1 suppresses metastatic features of cancer cells by compromising *KHPS1*- and eRNA-Sphk1-dependent expression of SPHK1.

Previous studies have suggested that eRNAs enhance transcription by stabilizing CTCF-mediated enhancer-promoter interactions (Kim et al., 2015; Werner et al., 2017). Inspection of chromatin immunoprecipitation sequencing (ChIP-seq) data deposited in the Encyclopedia of DNA Elements (ENCODE) database revealed the presence of a CTCF binding site in the first intron

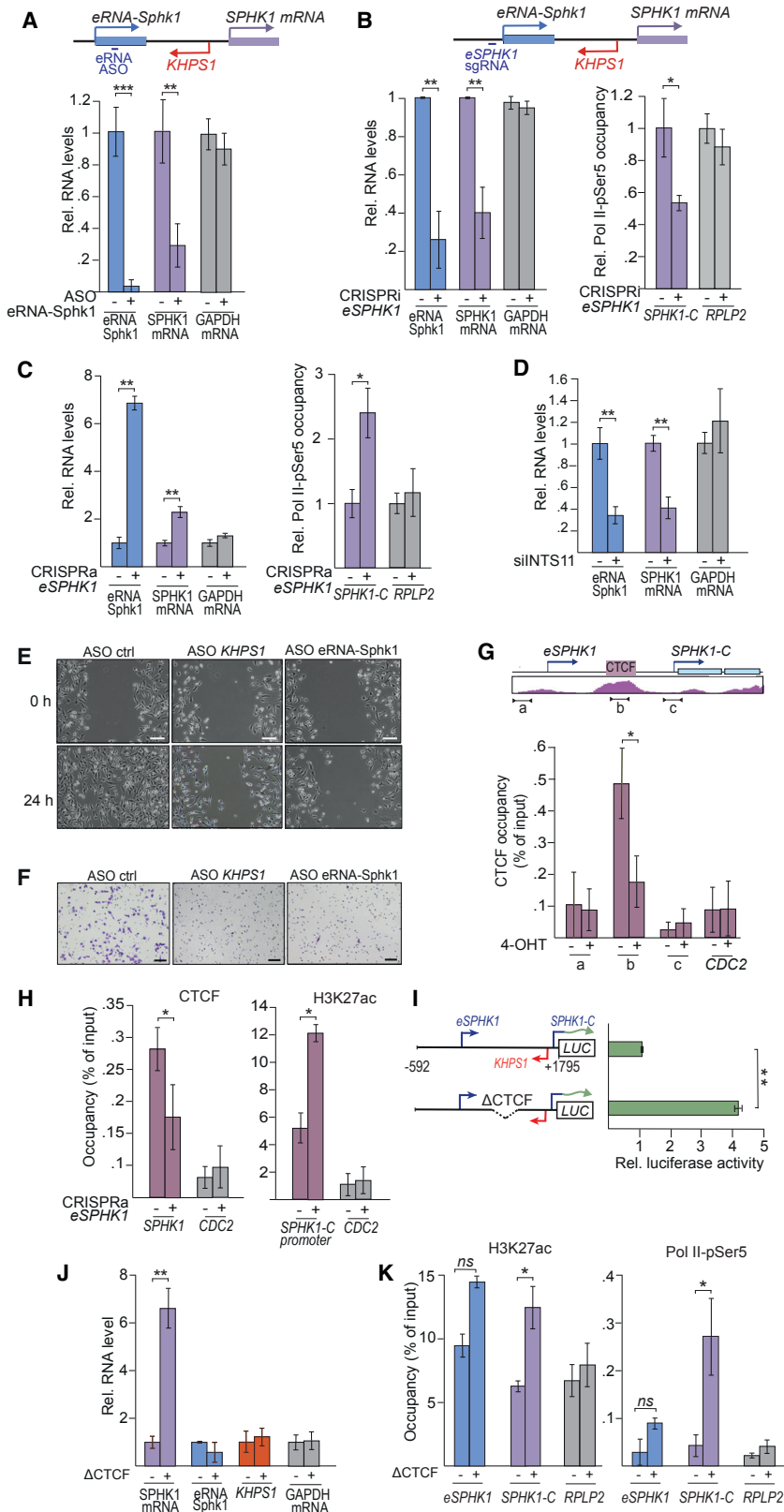


**Figure 2. eRNA-Sphk1 Stimulates Transcription of SPHK1-C by Evicting CTCF**

(A) Levels of eRNA-Sphk1, SPHK1 mRNA, and GAPDH mRNA upon transfection with non-specific ASO (-) or ASO targeting eRNA-Sphk1 (+352/+362) (+) (N = 3).

(B) Left: qRT-PCR showing levels of eRNA-Sphk1, SPHK1 mRNA, and GAPDH mRNA in U2OS/ER-E2F1 cells expressing dCas9-KRAB and sgRNA targeting either eSPHK1 (-20/-1) (+) or a non-specific sgRNA (-) (N = 3). Right: ChIP showing occupancy of initiating Pol II (Pol II-pSer5) at the *SPHK1-C* promoter normalized to total Pol II. Binding to the *RPLP2* promoter was monitored as control (N = 3).

(C) Left: qRT-PCR showing levels of eRNA-Sphk1, SPHK1 mRNA, and GAPDH mRNA in U2OS/ER-E2F1 cells expressing dCas9-VP64 and sgRNAs as in (B) (N = 3). Right: ChIP of initiating Pol II (Pol II-pSer5) at the *SPHK1-C* and *RPLP2* promoter analyzed as in (B) (N = 3).

(D) Levels of eRNA-Sphk1, SPHK1 mRNA, and GAPDH mRNA in 4-OHT-induced U2OS/ER-E2F1 cells transfected with siRNA against INTS11 (+) or control siRNA (-) (N = 3).

(E) Wound-healing assay in MDA-MB-231 cells transfected with a control ASO (ctrl) or with ASOs targeting *KHPS1* (-101/-121) or eRNA-Sphk1 (+352/+362). Gap closure was monitored 0 and 24 h after scratching by bright-field microscopy. Scale bars, 100  $\mu$ m.

(F) Cell invasion assay of MDA-MB-231 cells transfected as in (E). Scale bars, 100  $\mu$ m.

(G) Scheme: ChIP-seq track showing CTCF bound between the *SPHK1* enhancer and the *SPHK1-C* promoter in osteoblasts (GEO: GSM733784). The graph shows CTCF occupancy in untreated and 4-OHT-induced U2OS/ER-E2F1 cells. The regions analyzed by qPCR are -464/-698 (a), +638/+790 (b), and +1,658/+1,795 (c). Binding to the *CDC2* promoter was monitored as control (N = 3).

(H) ChIP showing occupancy of CTCF and H3K27ac in U2OS/ER-E2F1 cells co-transfected with a dCas9-VP64 expression vector and either eSPHK1-specific (+) or non-specific (-) sgRNAs. Binding to the *CDC2* promoter was monitored as control (N = 3).

(I) Reporter assay measuring expression of *SPHK1-C*-driven luciferase in U2OS/ER-E2F1 cells transfected with the indicated pREP4-luciferase plasmids and an E2F1 expression plasmid. Data are presented in reference to cells transfected with pREP4-SPHK1(-592/+1,795)-luc (N = 3).

(J) Levels of the indicated RNAs in parental U2OS/ER-E2F1 cells (wild-type [WT]) (-) or cells lacking the CTCF binding sites ( $\Delta$ CTCF) (+) between the TSS of eSPHK1 and the TSS of *SPHK1-C* after induction with 4-OHT (3 h) (N = 3).

(K) ChIP showing occupancy of H3K27ac and initiating Pol II at the eSPHK1 and *SPHK1-C* promoter in U2OS/ER-E2F1 cells as in (J). Binding to the *RPLP2* promoter was monitored as control (N = 3). Data are presented as mean  $\pm$  SEM. \*p < 0.05, \*\*p < 0.01, \*\*\*p < 0.001. ns, not significant. See also Figure S2.

of eRNA-Sphk1. To examine whether eRNA-Sphk1 transcription affects CTCF binding, we monitored CTCF occupancy in U2OS/ER-E2F1 before and after 4-OHT treatment. Induction of eRNA-Sphk1 by *KHPS1* led to decreased binding of CTCF to its target site located between *eSPHK1* and *SPHK1-C* (Figure 2G). Likewise, activation of eRNA-Sphk1 transcription by dCas9-VP64 led to decreased CTCF binding and enhanced H3K27ac occupancy at *SPHK1-C*, reinforcing that transcription of eRNA-Sphk1 triggers displacement of the CTCF insulator, thereby removing the boundary between *eSPHK1* and *SPHK1-C* (Figures 2H and S2L). Furthermore, reporter assays monitoring the promoter activity of *SPHK1-C* revealed a significant increase in plasmid-driven luciferase expression if the region comprising the CTCF binding site was deleted (Figure 2I). Finally, genomic deletion of the CTCF binding sites ( $\Delta$ CTCF) by CRISPR-Cas9 led to increased levels of *SPHK1* mRNA without affecting *KHPS1* or eRNA-Sphk1 transcription (Figures 2J and S2M). Enhanced transcription of *SPHK1* mRNA correlated with increased occupancy of Pol II and H3K27ac at the *SPHK1-C* promoter (Figure 2K). Collectively, these results indicate that transcription of eRNA-Sphk1 augments transcription of *SPHK1* mRNA by evicting CTCF that insulates the enhancer from the *SPHK1-C* promoter.

### Enhancer Activation Requires Binding of *KHPS1* to *eSPHK1*

Previous electrophoretic mobility shift assays (EMSAs) and capture experiments have shown that *KHPS1* is capable of binding to a stretch of homopurines within *eSPHK1*, forming a triple helical structure that anchors *KHPS1* to the *SPHK1* locus (Postepska-Igjielska et al., 2015). To investigate whether triplex formation is required for *KHPS1*-dependent activation of eRNA-Sphk1 transcription, we used a reporter plasmid (pTet-*KHPS1* (+1,448/–592)), which comprises a tetracycline-responsive promoter, the first exon of eRNA-Sphk1, and *eSPHK1* sequences (–592/+1) (Figure 3A). To assay reporter-derived transcripts rather than endogenous eRNA-Sphk1, the plasmid was transfected into NIH 3T3 cells and the readout of human eRNA-Sphk1 was monitored by qRT-PCR. Similar to upregulation of *KHPS1* by dCas9-VP64 or E2F1, doxycycline-induced transcription of *KHPS1* coincided with transcription activation of eRNA-Sphk1. Conversely, eRNA-Sphk1 synthesis was compromised after knockdown of *KHPS1* (Figures 3A and S3A). Thus, the reporter assay mimics the *in vivo* situation; that is, transcription of sense RNA depends on transcription of *KHPS1*.

To unambiguously prove that transcription of eRNA-Sphk1 requires tethering of *KHPS1* to the TFR of *SPHK1*, we abolished triplex formation by either deletion of the TFR or by inserting pyrimidine substitutions that impair Hoogsteen base pairing into the homopurine stretch. Sense transcription was not induced if the TFR was deleted ( $\Delta$ TFR) or if the TFR was mutated (mutTFR), emphasizing the importance of *KHPS1*-dependent triplex formation for activation of eRNA-Sphk1 (Figure 3B). Consistently, induction of *KHPS1* led to increased occupancy of E2F1 and p300 at the plasmid comprising an intact TFR, but not at plasmids in which the TFR was mutated or deleted (Figures 3C and S3B). These results emphasize that anchoring of *KHPS1* to the TFR is required for the recruitment of E2F1 and p300 and for eRNA-Sphk1 synthesis.

To further demonstrate the importance of the TFR for the association of *KHPS1* with *eSPHK1*, we incubated biotinylated *KHPS1* versions comprising wild-type, mutated, or deleted TFRs with corresponding DNA fragments and captured RNA-associated DNA on streptavidin beads. Consistent with the reporter assays, ectopic wild-type *KHPS1* captured the TFR-containing DNA fragment, while no binding was observed if the TFR was mutated or deleted (Figure 3D).

Given that p300/CBP interacts with RNA (Postepska-Igjielska et al., 2015; Bose et al., 2017), we sought to delineate the region of *KHPS1* that conveys the interaction with p300. To this end, we immunoprecipitated UV-crosslinked p300-RNA complexes from 4-OHT-treated U2OS/ER-E2F1 cells and monitored *KHPS1* association by qRT-PCR using primers that cover different regions of *KHPS1*. This experimental approach revealed that p300 preferentially bound to *KHPS1* sequences comprising the first exon of eRNA-Sphk1 (amplicon D), but not to sequences located upstream (amplicons A–C) or downstream (amplicons E–G) of exon 1 (Figure 3E). *HOTAIR* and 18S rRNA used as controls did not bind to p300, demonstrating that p300 binds to RNA in a sequence- or structure-dependent manner.

The finding that different regions of *KHPS1* bind to p300 and DNA indicates that *KHPS1* comprises distinct functional domains that govern the interaction with DNA and p300, respectively. To examine whether compromised binding of p300 to reporter plasmids lacking a functional TFR was due to perturbation of triplex formation, we monitored p300 binding to *KHPS1* by RNA immunoprecipitation (RIP) experiments. p300 was associated with reporter transcripts containing the wild-type, depleted, or mutated TFR sequence, but not with *KHPS1* lacking sequences within the first exon of eRNA-Sphk1 ( $\Delta$ +25/+193), which mediate the interaction with p300 (Figure 3F). Accordingly, deletion of this region compromised activation of eRNA-Sphk1 (Figure S3C). These results reinforce that tethering *KHPS1* to the TFR is necessary for the recruitment of p300 to *eSPHK1*, but not for the interaction of *KHPS1* with p300.

### Triplex Motifs Mediate Site-Specific Targeting of lncRNA-Associated Proteins

Next, we examined whether foreign sequences that have been reported to form RNA-DNA triplexes would be capable of functionally replacing the TFR of *eSPHK1* and activating reporter gene transcription. For this, we replaced the TFR of *eSPHK1* by TFR sequences of *Fendrr* (Grote et al., 2013), *MEG3*, or the *MEG3* target gene *TGFBR1* (Mondal et al., 2015) in the reporter plasmid pTet-*KHPS1*(+1,448/–592) (Figure 4A). After transfection and doxycycline treatment, all chimeric constructs yielded similar levels of *KHPS1*. Significantly, sense transcription was activated if the plasmids contained a genuine triplex-forming sequence, that is, the TFR of *eSPHK1*, *Fendrr*, *MEG3*, or *TGFBR1*. Constructs in which the TFR was replaced by control sequences, such as U2 small nuclear RNA (snRNA)- or luciferase-derived sequences, did not promote transcription of eRNA-Sphk1 (Figures 4B and S4A). Again, transcription was compromised upon ASO-mediated knockdown of chimeric *KHPS1*, demonstrating that transcripts harboring triplex-forming sequences are required for activation of eRNA-Sphk1 transcription (Figure S4B). Enhanced sense transcription correlated with

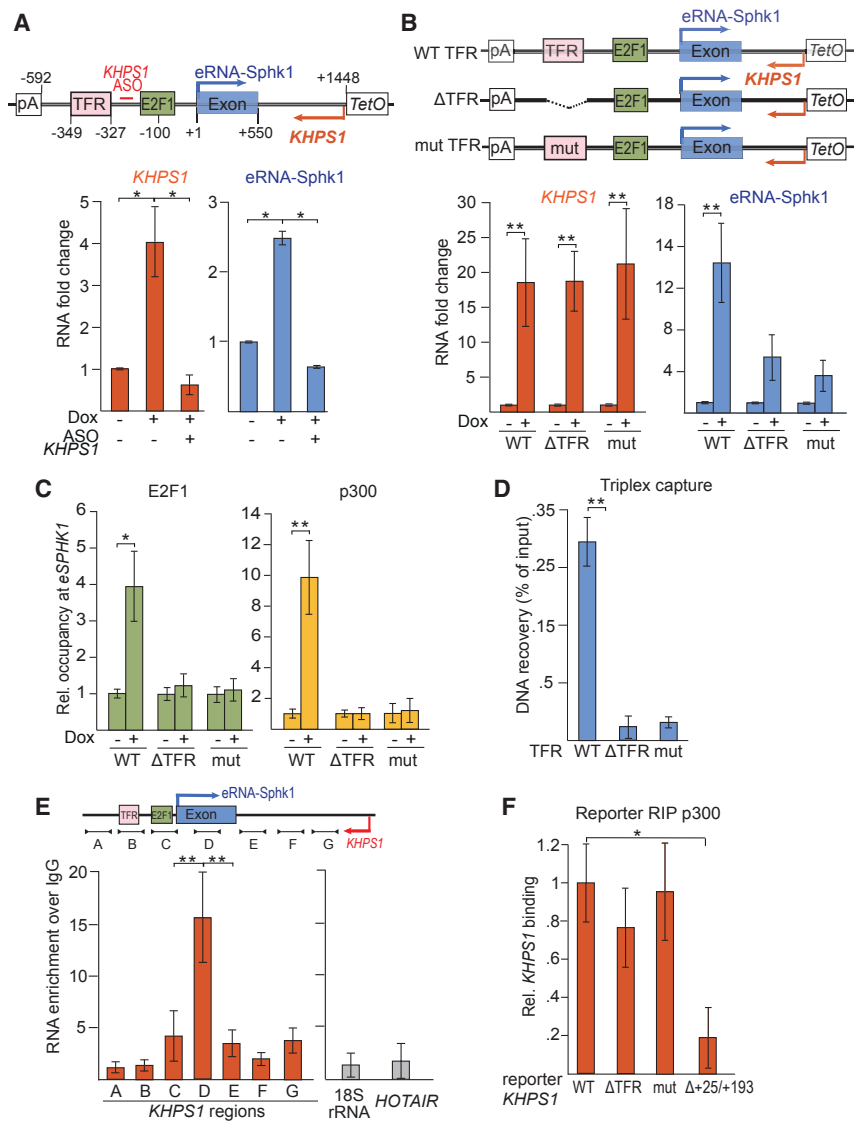


**Figure 3. Enhancer Activation Requires the Association of KHPS1 with eSPHK1**

(A) Levels of KHPS1 and eRNA-Sphk1 in NIH 3T3 Tet-ON cells transfected with the reporter plasmid pTet-KHPS1(+1,448/-592) and ASO targeting KHPS1 upon induction with doxycycline (3 μg/mL, 12 h) (N = 3). The scheme above presents the structure of pTet-KHPS1(+1,448/-592). Triplex-forming region (TFR) and E2F1 binding site are indicated (TetO, Tet promoter; pA, polyadenylation site).

(B) Levels of KHPS1 and eRNA-Sphk1 in NIH 3T3 Tet-ON cells transfected with the indicated reporter plasmids pTet-KHPS1(+1,448/-592). Cells were induced with doxycycline (5 μg/mL, 18 h) or left untreated (N = 4). The scheme above illustrates the structure of pTet-KHPS1(+1,448/-592) comprising the intact TFR of eSPHK1 (WT TFR), deleted TFR (ΔTFR), or mutated TFR (mutTFR) (TetO, Tet promoter; pA, polyadenylation site).

(C) ChIPs showing occupancy of E2F1 and p300 at pTet-KHPS1(+1,448/-592) as in (B). Binding was monitored by qPCR using primers -137/-89 (N = 3).

(D) Biotinylated KHPS1 (-373/-241) versions comprising the intact TFR (WT), ΔTFR, or mutTFR were incubated with a corresponding DNA fragment (-406/-65), and captured DNA was measured by qPCR (N = 3).

(E) Cross-linking and immunoprecipitation (CLIP)-qPCR monitoring binding of p300 to different regions of KHPS1 (A, -592/-425; B, -373/-304; C, -137/-89; D, +108/+165; E, +630/+790; F, +930/+1,124; and G, +1,132/+1,242). Binding to HOTAIR and 18S rRNA was monitored as control. RNA enrichment was calculated as a percentage of sample input and normalized to a percentage of input of the immunoglobulin G (IgG) (N = 4).

(F) RIP assay showing levels of reporter-derived KHPS1 associated with endogenous p300 in NIH 3T3 Tet-ON cells transfected with pTet-KHPS1(+1,448/-592) comprising the intact TFR (WT), ΔTFR, or mutTFR or lacking nucleotides +25/+193 relative to the eSPHK1 TSS (Δ+25/+193) (N = 3). Data are presented as mean ± SEM. \*p < 0.05, \*\*p < 0.01.

See also Figure S3.

increased occupancy of E2F1 and p300 at TFR-containing reporter plasmids (Figures 4C and S4C), reinforcing that foreign purine-rich sequences can functionally replace the TFR of eSPHK1 and facilitate recruitment of regulatory proteins.

To substantiate that RNAs containing the TFR of KHPS1 bind to eSPHK1 via Hoogsteen base pairing, we performed *in vitro* capture assays using biotinylated RNAs comprising the TFR of KHPS1, Fendrr, MEG3, and TGFBR1. U2 snRNA- or luciferase-derived sequences served as negative controls (Figure 4A). To distinguish triplex-mediated capturing from unspecific DNA binding, we used DNA fragments that were generated either in the presence of unmodified nucleotides or in the presence of 7-deaza-purine nucleotides, which do not allow Hoogsteen base pairing. After incubation of chimeric RNAs with corresponding DNA fragments and capturing on streptavidin-coated beads, RNA-associated DNA was monitored by PCR. The interaction between RNAs and DNA fragments containing the TFR of

eSPHK1, Fendrr, MEG3, or TGFBR1 was abolished when the PCR fragments were generated in the presence of 7-deaza-purine nucleotides (Figure 4D), validating that the association with DNA is brought about by Hoogsteen base pairing.

To validate the functional interchangeability of TFR motifs in targeting lncRNA-associated proteins to specific genomic loci, we transfected synthetic RNA harboring KHPS1 sequences from -406/+596 or a corresponding chimeric RNA in which the TFR of KHPS1 was replaced by the TFR of MEG3 (KHPS1-MEG3) and monitored H3K27ac and E2F1 occupancy at cellular SPHK1, MEG3, and TGFBR1. Ectopic RNA comprising the TFR of KHPS1 led to enhanced occupancy of E2F1 and H3K27ac at the SPHK1 locus, whereas KHPS1-MEG3 RNA did not affect occupancy of E2F1 and H3K27ac at eSPHK1. Conversely, ectopic KHPS1-MEG3 RNA, but not KHPS1, led to increased occupancy of E2F1 and higher levels of H3K27ac at endogenous TGFBR1 and MEG3 (Figures 4E and S4D). These RNA transfection



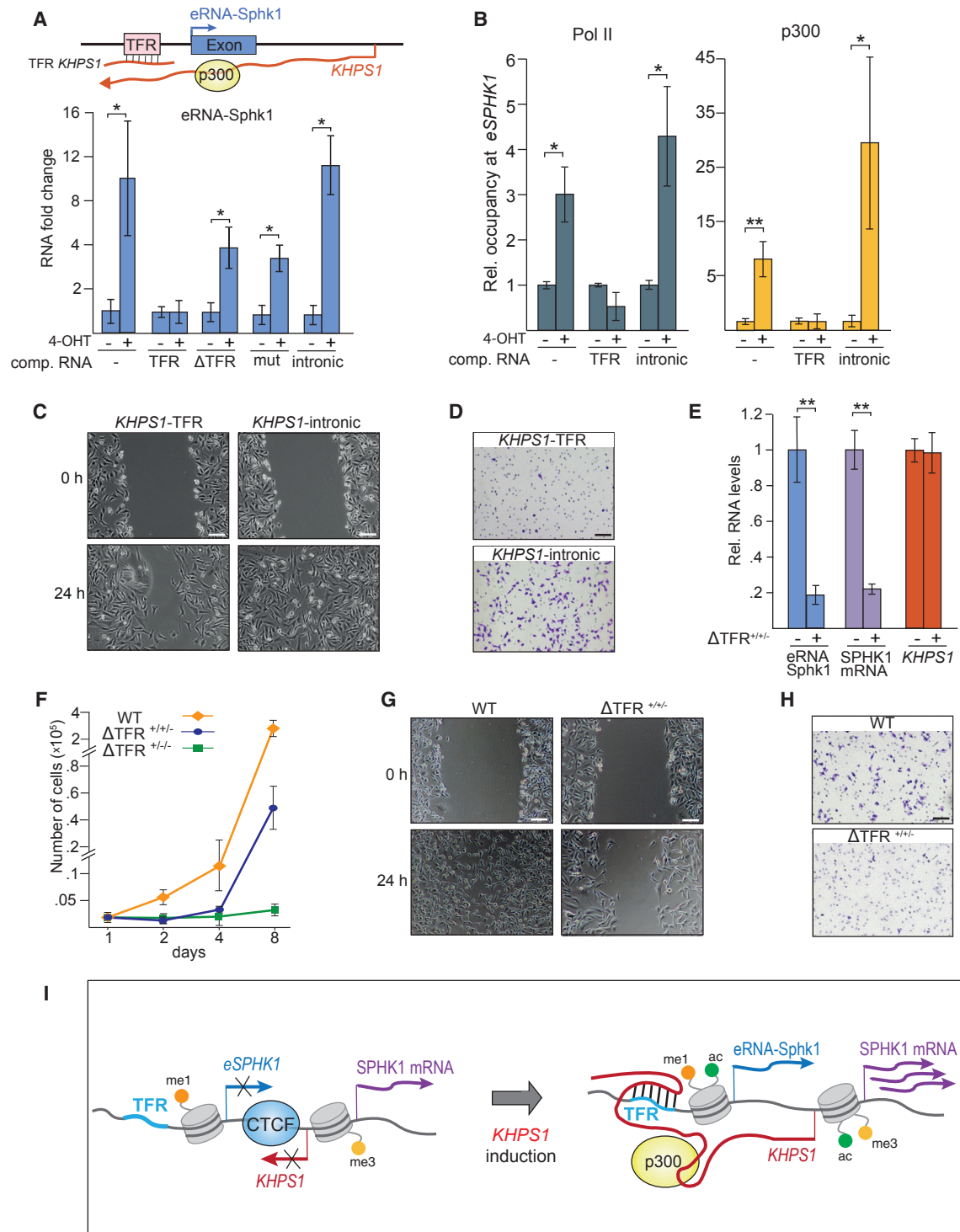


**Figure 5. Triplex Formation Is Indispensable for SPHK1 Expression**

(A) Experiment showing the level of eRNA-Sphk1 in untransfected (–) U2OS/ER-E2F1 cells or in cells transfected with synthetic KHPS1 (–373/–241) harboring intact TFR,  $\Delta$ TFR, or mutTFR or intronic sequences (+638/+790). eRNA-Sphk1 was induced with 4-OHT (2 h). The scheme illustrates the principle of the competition-based approach (N = 3).

(B) ChIP showing binding of Pol II and p300 to eSPHK1 in U2OS/ER-E2F1 cells upon transfection of RNA comprising the TFR (–373/–241) or intronic sequences (+638/+790) of KHPS1 (N = 3).

(legend continued on next page)

p300 at *eSPHK1* in 4-OHT-treated cells after transfection of TFR-containing RNA (Figures 5B and S5B). These results demonstrate that ectopic RNAs that contain the respective TFR sequence compete for binding of *KHPS1* to *eSPHK1*, reinforcing that binding of endogenous *KHPS1* to DNA is required for p300 recruitment and transcription of eRNA-Sphk1.

Because triplex-mediated anchoring of *KHPS1* is indispensable for enhancer activation and SPHK1 expression, we expected that the cellular tumorigenic potential would be compromised if the association of *KHPS1* with DNA were prevented. Wound healing, cell invasion, and colony formation were impaired after transfection of short synthetic RNA comprising the TFR (–373/–241), whereas intronic RNA did not affect these processes (Figures 5C, 5D, S5C, and S5D). These results underscore that the physical association of *KHPS1* with the TFR is essential for SPHK1-dependent downstream events.

To monitor the impact of triplex formation on SPHK1-dependent processes, we deleted a 66 bp genomic sequence comprising the TFR by CRISPR-Cas9. In haploid HAP1 cells, deletion of the TFR turned out to be lethal. To overcome the lethality caused by SPHK1 deficiency upon deletion of the TFR, we used MDA-MB-231 cells, which are triploid for chromosome 17 harboring *SPHK1*. Again, homozygous deletion of the TFR was lethal, substantiating the importance of the TFR for SPHK1 expression and cell viability. Even though the level of *KHPS1* was similar in all clones, both eRNA-Sphk1 and SPHK1 mRNA were markedly decreased in  $\Delta\text{TFR}^{+/+/-}$  clones harboring monoallelic TFR deletions (Figures 5E, S5E, and S5F), which correlated with decreased cell proliferation (Figure 5F). Biallelic deletion of the TFR ( $\Delta\text{TFR}^{+/-/-}$ ) impaired cell proliferation even more severely and led to cell death. Cells with monoallelic TFR deletion showed a considerable delay in gap closure and cell invasion assays, underscoring that anchoring *KHPS1* to the enhancer TFR is pivotal for SPHK1-dependent functions (Figures 5G and 5H). These experiments reveal a hierarchical regulatory cascade in which *KHPS1* tethered to the *eSPHK1* promotes transcription of eRNA-Sphk1, which in turn is a prerequisite for upregulation of SPHK1 mRNA and cell proliferation (Figure 5I).

## DISCUSSION

Although lncRNAs have been implicated in numerous cellular processes, their mode of action has mostly been linked to regu-

lation of protein coding genes. Here we provide evidence that lncRNAs can also activate poised enhancers to drive transcription of the respective target genes. We have previously reported that the antisense RNA *KHPS1* can form a triple helical structure at the promoter of *SPHK1-B* (Postepska-Igielska et al., 2015). Here we show that upon induction of *KHPS1*, the isoB promoter gains active enhancer-specific marks, such as p300 occupancy and H3K27ac, indicating that the *SPHK1-B* promoter is a poised enhancer that is activated by *KHPS1*. In support of this notion, the establishment of active histone marks correlated with increased levels of isoB transcripts, which exhibit characteristic features of eRNAs, such as nuclear localization, short half-life, and activation of specific target gene(s). Moreover, induction of eRNA-Sphk1 by dCas9-VP64 increased transcription of *SPHK1-C*. Conversely, ASO- and CRISPR interference (CRISPRi)-mediated downregulation of eRNA-Sphk1 led to compromised transcription of SPHK1 mRNA, indicating that both enhancer transcription and eRNA-Sphk1 are required for activation of *SPHK1-C*.

eRNAs have been proposed to regulate gene expression by mediating enhancer-promoter interaction via DNA loops and by association with chromatin-modifying enzymes that establish a transcription-permissive chromatin structure (Kim et al., 2015; Werner et al., 2017). Our results uncover another function of eRNA; that is, transcription of eRNA leads to eviction of CTCF, which insulates *eSPHK1* from the *SPHK1-C* promoter. Numerous studies have shown that CTCF facilitates enhancer-promoter interactions; however, the mechanism underlying the enhancer-blocking activity of CTCF remained elusive. Our study shows that eRNA-Sphk1 displaces CTCF, which in turn leads to activation of SPHK1 mRNA transcription. Given that the human genome contains thousands of CTCF binding sites and many enhancers produce eRNA, transcription of enhancer RNA may represent a common mechanism allowing neighboring genes to be differentially regulated (Bell et al., 1999; Xie et al., 2007; Ren et al., 2017).

Triplex-forming motifs are widespread in mammalian genomes; on average, there is one specific TFR every 1.6 kb in the human genome, located preferentially at regulatory elements (Buske et al., 2012). Thus, tethering lncRNAs to DNA via triplex formation may represent a general mechanism for target gene recognition of chromatin-modifying enzymes and transcription regulators. Several studies have proposed that lncRNAs can

(C) Wound-healing assay in MDA-MB-231 cells transfected with *KHPS1* versions comprising the TFR (–373/–241) or intronic sequences (+638/+790). Gap closure was monitored 0 and 24 h after scratching by bright-field microscopy. Scale bars, 100  $\mu\text{m}$ .

(D) Cell invasion assay of MDA-MB-231 cells transfected as in (C). Scale bars, 100  $\mu\text{m}$ .

(E) Levels of eRNA-Sphk1, SPHK1 mRNA, and *KHPS1* in parental cells (–) and in mutant MDA-MB-231 cells comprising a monoallelic TFR deletion ( $\Delta\text{TFR}^{+/+/-}$ ) (+) (N = 3).

(F) Proliferation of parental cells (WT) and mutant MDA-MB-231 cells comprising a monoallelic TFR deletion ( $\Delta\text{TFR}^{+/+/-}$ ) or biallelic TFR deletion ( $\Delta\text{TFR}^{+/-/-}$ ) (N = 3).

(G) Scratch assay performed with WT and  $\text{TFR}^{+/+/-}$  MDA-MB-231 cells. Gap closure was monitored 0 and 24 h after scratching by bright-field microscopy. Scale bars, 100  $\mu\text{m}$ .

(H) Cell invasion assay using WT and  $\Delta\text{TFR}^{+/+/-}$  MDA-MB-231 cells. Scale bars, 100  $\mu\text{m}$ .

(I) Model of *KHPS1*-dependent regulation of SPHK1 mRNA transcription. *KHPS1* tethered to the TFR of the *SPHK1* enhancer (*eSPHK1*) via RNA-DNA triplex formation recruits p300 and activates the synthesis of eRNA-Sphk1. eRNA-Sphk1 evicts CTCF, which insulates *eSPHK1* from *SPHK1-C* and augments transcription of SPHK1 mRNA.

Data are presented as mean  $\pm$  SEM unless specified differently. \*p < 0.05, \*\*p < 0.01.

See also Figure S5.

form triplexes with regulatory DNA elements. Examples are pRNA, a nucleolar RNA originating from the intergenic spacer, which forms RNA-DNA triplexes at the rDNA promoter (Schmitz et al., 2010). PAPAS, a nucleolar lncRNA that is transcribed in antisense orientation to pre-rRNA, facilitates recruitment of the CHD4/NuRD repressor to rDNA (Zhao et al., 2016, 2018). Other examples of triplex-forming lncRNAs are *PARTICLE*, which affects the expression of *MAT2A* (O'Leary et al., 2015); *Fendrr*, which recruits the PRC2 complex to developmental genes (Grote et al., 2013); *MEG3*, which guides PRC2 to TGF- $\beta$ -responsive genes (Mondal et al., 2015); and *HOTAIR*, which regulates adipogenic differentiation of mesenchymal stem cells (Kalwa et al., 2016).

A key issue of the present study was to unequivocally prove that transcription activation of *SPHK1* requires anchoring of *KHPS1* to the TFR at the *eSPHK1*. If the TFR was deleted or perturbed by pyrimidine interruptions, elevated levels of *KHPS1* increased neither the occupancy of E2F1 and p300 nor the transcription of sense RNA. This result demonstrates that tethering of *KHPS1* to the enhancer TFR is essential for targeting regulatory proteins complexes to *eSPHK1* and activation of eRNA transcription. The importance of triplex formation for *KHPS1*-dependent transcription activation was substantiated by swap experiments in which the TFR of the reporter plasmid was replaced by foreign sequences that were reported to be engaged in triplex formation. Substitution of the TFR of *SPHK1* with triplex-forming sequences present in *Fendrr* (Grote et al., 2013) or in *MEG3* or its target gene *TGFBR1* (Mondal et al., 2015) functionally replaced the TFR of *SPHK1*; that is, chimeric *KHPS1* comprising foreign TFRs was capable of binding to the respective DNA sequence and mediating activation of sense transcription at the reporter. Replacement of the TFR of *KHPS1* by the TFR of *MEG3* led to increased occupancy of H3K27ac and E2F1 at endogenous *TGFBR1*, a gene that is targeted by *MEG3*. This result emphasizes the importance of triplex formation in lncRNA-mediated targeting of regulatory proteins to remote genomic sites.

The functional importance of triplex formation for *KHPS1*-dependent expression of *SPHK1* was further documented by competition experiments. Transfection of a short synthetic RNA comprising the TFR of *KHPS1* efficiently competed for binding of endogenous *KHPS1* to the *eSPHK1*. As a consequence, expression of eRNA-Sphk1 was attenuated, leading to impaired cell migration, invasion, and clonogenicity. Furthermore, homozygous genomic deletion of the TFR turned out to be lethal. Mono- or biallelic deletion of the TFR in MD-MBA-231 cells severely impaired cell viability. Depletion of *KHPS1* or eRNA-Sphk1 led to decreased cell migration, invasion, and colony formation of MD-MBA-231 cells, indicating that downregulation of these lncRNAs compromises the malignant phenotype. Altogether, we have provided compelling evidence that transcription of both eRNA-Sphk1 and *SPHK1* mRNA depends on the physical association of *KHPS1* with the *eSPHK1* (Figure 5). Although we have yet to understand how RNA-DNA triplex formation is regulated, our results suggest that triplex-based recruitment of chromatin-modifying complexes may represent a common targeting mechanism for transcription regulators bound to lncRNAs.

## STAR★METHODS

Detailed methods are provided in the online version of this paper and include the following:

- KEY RESOURCES TABLE
- CONTACT FOR REAGENT AND RESOURCE SHARING
- EXPERIMENTAL MODEL AND SUBJECT DETAILS
- METHOD DETAILS
  - Cell transfection and treatments
  - Recombinant plasmids preparation
  - RNA isolation and quantitative RT-PCR
  - Luciferase assay
  - Chromatin immunoprecipitation (ChIP)
  - RNA immunoprecipitation (RIP)
  - Cross-linking and immunoprecipitation (CLIP) assay
  - Triplex Capture Assay
  - Wound-healing and invasion assays
  - Soft agar colony formation assay
- QUANTIFICATION AND STATISTICAL ANALYSIS

## SUPPLEMENTAL INFORMATION

Supplemental Information can be found with this article online at <https://doi.org/10.1016/j.celrep.2019.02.059>.

## ACKNOWLEDGMENTS

We thank all group members for helpful discussions and support. We are grateful to Doron Ginsberg (Bar Ilan University, Ramat Gan, Israel) for providing U2OS/ER-E2F1 cells and Christina Maul for technical assistance. This work was supported by the Deutsche Forschungsgemeinschaft (GR475/22-1 and SFB1036), the Baden-Württemberg Stiftung (NCRNA\_025), the Cooperation Program in Cancer Research of the Deutsches Krebsforschungszentrum (DKFZ), and Israel's Ministry of Science, Technology and Space (MOST).

## AUTHOR CONTRIBUTIONS

A.B.-G. and A.P.-I. carried out experiments and analyzed the data. I.G. conceived and supervised the project. All authors contributed to writing the manuscript.

## DECLARATION OF INTERESTS

The authors declare no competing interests.

Received: May 8, 2018

Revised: November 14, 2018

Accepted: February 14, 2019

Published: March 12, 2019

## REFERENCES

- Bell, A.C., West, A.G., and Felsenfeld, G. (1999). The protein CTCF is required for the enhancer blocking activity of vertebrate insulators. *Cell* 98, 387–396.
- Bose, D.A., Donahue, G., Reinberg, D., Shiekhattar, R., Bonasio, R., and Berger, S.L. (2017). RNA Binding to CBP Stimulates Histone Acetylation and Transcription. *Cell* 168, 135–149.
- Buske, F.A., Bauer, D.C., Mattick, J.S., and Bailey, T.L. (2012). Triplexator: detecting nucleic acid triple helices in genomic and transcriptomic data. *Genome Res.* 22, 1372–1381.
- Chen, X., Sun, Y., Cai, R., Wang, G., Shu, X., and Pang, W. (2018). Long non-coding RNA: multiple players in gene expression. *BMB Rep.* 51, 280–289.

- Datta, A., Loo, S.Y., Huang, B., Wong, L., Tan, S.S.L., Tan, T.Z., Lee, S.-C., Thiery, J.P., Lim, Y.C., Yong, W.P., et al. (2014). SPHK1 regulates proliferation and survival responses in triple-negative breast cancer. *Oncotarget* 5, 5920–5933.
- De Santa, F., Barozzi, I., Mietton, F., Ghisletti, S., Polletti, S., Tusi, B.K., Muller, H., Ragoussis, J., Wei, C.L., and Natoli, G. (2010). A large fraction of extragenic RNA pol II transcription sites overlap enhancers. *PLoS Biol.* 8, e1000384.
- Felsenfeld, G., Davies, D.R., and Rich, A. (1957). Formation of a three-stranded polynucleotide molecule. *J. Am. Chem. Soc.* 79, 2023–2024.
- French, K.J., Schrecengost, R.S., Lee, B.D., Zhuang, Y., Smith, S.N., Eberly, J.L., Yun, J.K., and Smith, C.D. (2003). Discovery and evaluation of inhibitors of human sphingosine kinase. *Cancer Res.* 63, 5962–5969.
- Gilbert, L.A., Larson, M.H., Morsut, L., Liu, Z., Brar, G.A., Torres, S.E., Stern-Ginossar, N., Brandman, O., Whitehead, E.H., Doudna, J.A., et al. (2013). CRISPR-mediated modular RNA-guided regulation of transcription in eukaryotes. *Cell* 154, 442–451.
- Goñi, J.R., de la Cruz, X., and Orozco, M. (2004). Triplex-forming oligonucleotide target sequences in the human genome. *Nucleic Acids Res.* 32, 354–360.
- Grote, P., Wittler, L., Hendrix, D., Koch, F., Währisch, S., Beisaw, A., Macura, K., Bläss, G., Kellis, M., Werber, M., and Herrmann, B.G. (2013). The tissue-specific lncRNA Fendrr is an essential regulator of heart and body wall development in the mouse. *Dev. Cell* 24, 206–214.
- Hershko, T., Chaussepied, M., Oren, M., and Ginsberg, D. (2005). Novel link between E2F and p53: proapoptotic cofactors of p53 are transcriptionally up-regulated by E2F. *Cell Death Differ.* 12, 377–383.
- Hsieh, C.-L., Fei, T., Chen, Y., Li, T., Gao, Y., Wang, X., Sun, T., Sweeney, C.J., Lee, G.-S.M., Chen, S., et al. (2014). Enhancer RNAs participate in androgen receptor-driven looping that selectively enhances gene activation. *Proc. Natl. Acad. Sci. USA* 111, 7319–7324.
- Imamura, T., Yamamoto, S., Ohgane, J., Hattori, N., Tanaka, S., and Shiota, K. (2004). Non-coding RNA directed DNA demethylation of Sphk1 CpG island. *Biochem. Biophys. Res. Commun.* 322, 593–600.
- Kalwa, M., Hänzelmann, S., Otto, S., Kuo, C.C., Franzen, J., Jousen, S., Fernandez-Rebollo, E., Rath, B., Koch, C., Hofmann, A., et al. (2016). The lncRNA HOTAIR impacts on mesenchymal stem cells via triple helix formation. *Nucleic Acids Res.* 44, 10631–10643.
- Kim, T.K., Hemberg, M., Gray, J.M., Costa, A.M., Bear, D.M., Wu, J., Harmin, D.A., Laptewicz, M., Barbara-Haley, K., Kuersten, S., et al. (2010). Widespread transcription at neuronal activity-regulated enhancers. *Nature* 465, 182–187.
- Kim, Y.W., Lee, S., Yun, J., and Kim, A. (2015). Chromatin looping and eRNA transcription precede the transcriptional activation of gene in the  $\beta$ -globin locus. *Biosci. Rep.* 35, 1–8.
- Lai, F., Gardini, A., Zhang, A., and Shiekhattar, R. (2015). Integrator mediates the biogenesis of enhancer RNAs. *Nature* 525, 399–403.
- Lam, M.T.Y., Li, W., Rosenfeld, M.G., and Glass, C.K. (2014). Enhancer RNAs and regulated transcriptional programs. *Trends Biochem. Sci.* 39, 170–182.
- Li, W., Notani, D., Ma, Q., Tanasa, B., Nunez, E., Chen, A.Y., Merkurjev, D., Zhang, J., Ohgi, K., Song, X., et al. (2013). Functional roles of enhancer RNAs for oestrogen-dependent transcriptional activation. *Nature* 498, 516–520.
- Li, Y., Syed, J., and Sugiyama, H. (2016). RNA-DNA triplex formation by long noncoding RNAs. *Cell Chem. Biol.* 23, 1325–1333.
- Long, Y., Wang, X., Youmans, D.T., and Cech, T.R. (2017). How do lncRNAs regulate transcription? *Sci. Adv.* 3, eaao2110.
- Marcu, M.G., Jung, Y.-J., Lee, S., Chung, E.-J., Lee, M.-J., Trepel, J., and Neckers, L. (2006). Curcumin is an inhibitor of p300 histone acetyltransferase. *Med. Chem.* 2, 169–174.
- Mondal, T., Subhash, S., Vaid, R., Enroth, S., Uday, S., Reinius, B., Mitra, S., Mohammed, A., James, A.R., Hoberg, E., et al. (2015). MEG3 long noncoding RNA regulates the TGF- $\beta$  pathway genes through formation of RNA-DNA triplex structures. *Nat. Commun.* 6, 7743.
- O’Leary, V.B., Ovsepiyan, S.V., Carrascosa, L.G., Buske, F.A., Radulovic, V., Niyazi, M., Moertl, S., Trau, M., Atkinson, M.J., and Anastasov, N. (2015). PARTICLE, a triplex-forming long ncRNA, regulates locus-specific methylation in response to low-dose irradiation. *Cell Rep.* 11, 474–485.
- Ørom, U.A., Derrien, T., Beringer, M., Gumireddy, K., Gardini, A., Bussotti, G., Lai, F., Zytznicki, M., Notredame, C., Huang, Q., et al. (2010). Long noncoding RNAs with enhancer-like function in human cells. *Cell* 143, 46–58.
- Paugh, B.S., Bryan, L., Paugh, S.W., Wilczynska, K.M., Alvarez, S.M., Singh, S.K., Kapitonov, D., Rokita, H., Wright, S., Griswold-Prenner, I., et al. (2009). Interleukin-1 regulates the expression of sphingosine kinase 1 in glioblastoma cells. *J. Biol. Chem.* 284, 3408–3417.
- Paugh, S.W., Coss, D.R., Bao, J., Lauder milk, L.T., Grace, C.R., Ferreira, A.M., Waddell, M.B., Ridout, G., Naeve, D., Leuze, M., et al. (2016). MicroRNAs form triplexes with double stranded DNA at sequence-specific binding sites; a eukaryotic mechanism via which microRNAs could directly alter gene expression. *PLoS Comput. Biol.* 12, e1004744.
- Postepska-Igielska, A., Giwojna, A., Gasri-Plotnitsky, L., Schmitt, N., Dold, A., Ginsberg, D., and Grummt, I. (2015). LncRNA Khps1 regulates expression of the proto-oncogene SPHK1 via triplex-mediated changes in chromatin structure. *Mol. Cell* 60, 626–636.
- Radziszewska, A., Shlyueva, D., Müller, I., and Helin, K. (2016). Optimizing sgRNA position markedly improves the efficiency of CRISPR/dCas9-mediated transcriptional repression. *Nucleic Acids Res.* 44, e141.
- Ren, C., Liu, F., Ouyang, Z., An, G., Zhao, C., Shuai, J., Cai, S., Bo, X., and Shu, W. (2017). Functional annotation of structural ncRNAs within enhancer RNAs in the human genome: implications for human disease. *Sci. Rep.* 7, 15518.
- Sarkar, S., Maceyka, M., Hait, N.C., Paugh, S.W., Sankala, H., Milstien, S., and Spiegel, S. (2005). Sphingosine kinase 1 is required for migration, proliferation and survival of MCF-7 human breast cancer cells. *FEBS Lett.* 579, 5313–5317.
- Schmitz, K.M., Mayer, C., Postepska, A., and Grummt, I. (2010). Interaction of noncoding RNA with the rDNA promoter mediates recruitment of DNMT3b and silencing of rRNA genes. *Genes Dev.* 24, 2264–2269.
- Soibam, B. (2017). Super-lncRNAs: identification of lncRNAs that target super-enhancers via RNA:DNA:DNA triplex formation. *RNA* 23, 1729–1742.
- Thomas, M., White, R.L., and Davis, R.W. (1976). Hybridization of RNA to double-stranded DNA: formation of R-loops. *Proc. Natl. Acad. Sci. USA* 73, 2294–2298.
- Werner, M.S., Sullivan, M.A., Shah, R.N., Nadadur, R.D., Grzybowski, A.T., Galat, V., Moskowitz, I.P., and Ruthenburg, A.J. (2017). Chromatin-enriched lncRNAs can act as cell-type specific activators of proximal gene transcription. *Nat. Struct. Mol. Biol.* 24, 596–603.
- Xie, X., Mikkelsen, T.S., Gnirke, A., Lindblad-Toh, K., Kellis, M., and Lander, E.S. (2007). Systematic discovery of regulatory motifs in conserved regions of the human genome, including thousands of CTCF insulator sites. *Proc. Natl. Acad. Sci. USA* 104, 7145–7150.
- Zhao, Z., Dammert, M.A., Grummt, I., and Bierhoff, H. (2016). lncRNA-Induced Nucleosome Repositioning Reinforces Transcriptional Repression of rRNA Genes upon Hypotonic Stress. *Cell Rep* 14, 1876–1882.
- Zhao, Z., Sentürk, N., Song, C., and Grummt, I. (2018). lncRNA PAPAS tethered to the rDNA enhancer recruits hypophosphorylated CHD4/NuRD to repress rRNA synthesis at elevated temperatures. *Genes Dev.* 32, 836–848.
- Zhu, L., Wang, Z., Lin, Y., Chen, Z., Liu, H., Chen, Y., Wang, N., and Song, X. (2015). Sphingosine kinase 1 enhances the invasion and migration of non-small cell lung cancer cells via the AKT pathway. *Oncol. Rep.* 33, 1257–1263.

## STAR★METHODS

### KEY RESOURCES TABLE

REAGENT or RESOURCE	SOURCE	IDENTIFIER
<b>Antibodies</b>		
Mouse monoclonal anti-E2F1 (ChIP)	Santa Cruz	Cat# sc-251, RRID:AB_627476
Mouse monoclonal anti-p300 (ChIP)	Abcam	Cat# ab14984; RRID:AB_301550
Rabbit polyclonal anti- RNA Pol II (N-20) (ChIP)	Santa Cruz	Cat# sc-899, RRID:AB_632359
Mouse monoclonal anti- RNA Pol II CTD (ChIP)	Abcam	Cat# ab5408, RRID:AB_304868
Rabbit polyclonal anti-trimethyl-Histone H3 (Lys4) (ChIP)	Millipore	Cat# 07-473, RRID:AB_1977252
Rabbit polyclonal anti-Histone H3 (acetyl K27) (ChIP)	Abcam	Cat# ab4729, RRID:AB_2118291
Rabbit polyclonal anti-H3 (ChIP)	Diagenode	Cat# C15310135
Rabbit polyclonal anti-monomethyl Histone H3 (Lys4) (ChIP)	Millipore	Cat# 07-436, RRID:AB_10068114
Rabbit polyclonal anti-Histone H3 (tri methyl K27) (ChIP)	Abcam	Cat# ab195477
Rabbit polyclonal anti-CTCF (ChIP)	Active Motif	Cat# 61311, RRID:AB_2614975
Rabbit monoclonal anti-SPHK1 (WB)	Cell Signaling	Cat# 12071
Peroxidase AffiniPure Goat anti-Rabbit IgG (WB)	Dianova	Cat# 111-035-144, RRID:AB_2307391
Peroxidase AffiniPure Goat anti-Mouse IgG (WB)	Dianova	Cat# 115-035-062, RRID:AB_2338504
<b>Chemicals, Peptides, and Recombinant Proteins</b>		
4-hydroxytamoxifen	Sigma-Aldrich	Cat# H7904
SKI II	Sigma-Aldrich	Cat# S5696
Flavopiridol	Sigma-Aldrich	Cat# F3055
Doxycyclin	Sigma-Aldrich	Cat# D9891
Nicotinamide (NAM)	Sigma-Aldrich	Cat# N3376
Curcumin	Sigma-Aldrich	Cat# 239802
Crystal violet	Sigma-Aldrich	Cat# C0775
<b>Critical Commercial Assays</b>		
TRI-reagent	Sigma-Aldrich	Cat# T9424
Dual Luciferase Assay System	Promega	Cat# E4030
Transcriptor first strand cDNA synthesis kit	Roche	Cat# 0437901001
TURBO DNase	Ambion	Cat# AM2238
QuantiTect SYBR Green PCR Kit	QIAGEN	Cat# 204145
MEGAscript T7 Transcription Kit	Ambion	Cat# AM1334
PwoSuperYield DNA polymerase Kit	Roche	Cat# 4340868001
Lipofectamine 2000	ThermoFisher Scientific	Cat# 11668019
Lipofectamine 3000	ThermoFisher Scientific	Cat# L3000008
Lipofectamine RNA iMAX	ThermoFisher Scientific	Cat# 13778075
Exol restriction enzyme	New England Biolab	Cat# M0568
RNase I	ThermoFisher Scientific	Cat# EN0601
RNase A	Promega	Cat# EN0531
<b>Experimental Models: Cell Lines</b>		
Human U2OS/ER-E2F1 cell line	Ginsbergs lab, <a href="#">Hershko et al., 2005</a>	N/A
Human MDA-MB-231 cell line	ATCC	HTB-26
Human HeLa cell line	ATCC	N/A
Mouse NIH 3T3 Tet-ON cell line	Takara	Cat# 631197
<b>Oligonucleotides</b>		
ASO used in knockdown experiments, see <a href="#">Table S1</a>	This study	N/A
Oligonucleotides used for CRISPR-mediated mutagenesis, see <a href="#">Table S2</a>	This study	N/A

(Continued on next page)

**Continued**

REAGENT or RESOURCE	SOURCE	IDENTIFIER
Primers used in qPCR, see <a href="#">Table S3</a>	This study and <a href="#">Postepska-Igielska et al., 2015</a>	N/A
Primers used for strand-specific RT-qPCR, see <a href="#">Table S3</a>	This study	N/A
Primers used to generate transcription templates, see <a href="#">Table S3</a>	This study and <a href="#">Postepska-Igielska et al., 2015</a>	N/A
Oligonucleotides used for reporter plasmids with foreign TFRs, see <a href="#">Table S4</a>	This study	N/A
Sip300 SMARTpool: ON-TARGETplus EP300 siRNA	Dharmacon	Cat# L-003486-00
SiE2F1 SMARTpool: ON-TARGETplus E2F1 siRNA	Dharmacon	Cat# L-003259-00
siPCAF ON-TARGETplus Human KAT2A siRNA	Dharmacon	Cat# L-009722-02
<b>Recombinant DNA</b>		
pTet-KHPS1(+1448/-592)	<a href="#">Postepska-Igielska et al., 2015</a>	N/A
pTet-KHPS1(+1448/-592)mutTFR	This study	N/A
pTet-KHPS1(+1448/-592) $\Delta$ TFR	This study	N/A
pTet-KHPS1(+1448/-592)MEG3	This study	N/A
pTet-KHPS1(+1448/-592)TGFBF1	This study	N/A
pTet-KHPS1(+1448/-592)Fendrr	This study	N/A
pTet-KHPS1(+1448/-592)scrU2	This study	N/A
pTet-KHPS1(+1448/-592)scrLuc	This study	N/A
pGL4.10[luc2]	Promega	Cat# E6651, #9PIE665
pREP4 (pCEP4 with RSV promoter)	ThermoFisher Scientific	Cat# V004450
pREP4-SPHK1(-592/+1795)	This study	N/A
pREP4-SPHK1(+46/+1795)	This study	N/A
pREP4-SPHK1(-592/+1795) $\Delta$ CTCF	This study	N/A
pTet-7B-MS2bs-luc	This study	N/A
pTet-KHPS1(+1448/-592-IsoB-luc)	This study	N/A
pHAGE EF1 $\alpha$ dCas9-KRAB	Addgene	Cat# 50919
lentiGuide-Puro	Addgene	Cat# 52963
dCas9-VP64_GFP	Addgene	Cat# 61422
MS2-P65-HSF1_GFP	Addgene	Cat# 61423
sgRNA(MS1) cloning backbone	Addgene	Cat# 61424
lentiCRISPR v2	Addgene	Cat# 52961
<b>Software and Algorithms</b>		
Open Reading Frame Finder		<a href="https://www.ncbi.nlm.nih.gov/orffinder/">https://www.ncbi.nlm.nih.gov/orffinder/</a>
<b>Other</b>		
Dynabeads Protein-G	ThermoFisher Scientific	Cat# 10003D
Dynabeads MyOne Streptavidin C1	ThermoFisher Scientific	Cat# 65001
7-deaza-dGTP	Sigma-Aldrich	Cat# 10988537001
7-deaza-dATP	Tri-Link	Cat# N-2010

**CONTACT FOR REAGENT AND RESOURCE SHARING**

Further information and requests for reagents may be directed to and will be fulfilled by the Lead Contact, Ingrid Grummt ([i.grummt@dkfz-heidelberg.de](mailto:i.grummt@dkfz-heidelberg.de)).

**EXPERIMENTAL MODEL AND SUBJECT DETAILS**

HeLa (female), MDA-MB-231 (female) and NIH 3T3-TetON (male) cell lines grown in Dulbecco's modified Eagle's medium supplemented with 10% Fetal Bovine Serum (FBS) and 1% penicillin-streptomycin. U2OS/ER-E2F1 cell line (female) was grown in Dulbecco's modified Eagle's medium supplemented with 5% Fetal Bovine Serum (FBS) and 1% penicillin-streptomycin. All cells

were maintained under standard growth conditions at 37°C and 5% CO<sub>2</sub> in a humidified atmosphere. MDA-MB-231ΔTFR cells or U2OS/ER-E2F1ΔCTCF cells were generated by CRISPR-Cas9-mediated mutagenesis. Cells were transfected with lentiCRISPR v2 vectors harboring single guide RNAs targeting either the TFR or the CTCF binding sites at *SPHK1* (Table S2). Single clones were retrieved after 72 h of puromycin selection (0.2–0.5 μg/ml), expanded and screened by PCR using primers –592F/+25R or +108F/+1448R. Deletion of the TFR and the putative CTCF binding sites was confirmed by sequencing.

## METHOD DETAILS

### Cell transfection and treatments

Lipofectamine 3000 was used for transfection of U2OS/ER-E2F1 cells with plasmid DNA and Lipofectamine RNAiMAX for transfection of RNA or siRNAs. For reporter assays, 3 × 10<sup>4</sup> NIH 3T3 Tet-ON cells were transfected with 2 ng of pTet-*KHPS1*(+1448/-592) using Lipofectamine 2000. Cells were replated after 24 h and induced with 5 μg/ml doxycycline for 16 h. To knockdown *KHPS1* or eRNA-Sphk1, cells were reverse-transfected twice with 20 μM ASOs using Lipofectamine RNAiMAX. Customly designed scrambled ASOs were used as a control. Cells were harvested 72 h after transfection and proceeded for RNA analysis. ASO sequences are listed in Table S1. For CRISPRi, 8 × 10<sup>4</sup> U2OS/ER-E2F1 cells were transfected with 100 ng of dCas9-KRAB and 100 ng of lentiGuide-Puro plasmid expressing sgRNAs that target *SPHK1-B* promoter. Cells were harvested 24 h after transfection. For CRISPRa, U2OS/ER-E2F1 cells were transfected with 50 ng of dCas9-VP64\_GFP, 50 ng of MS2-P65-HSF1\_GFP and 50 ng of sgRNA(MS2) expressing sgRNAs which target *SPHK1-B* or *KHPS1* promoters. Cells were harvested 24 h after transfection. Sequences of sgRNAs are listed in Table S2.

For activation of ER-tagged E2F1, U2OS/ER-E2F1 cells were treated with 100 nM 4-hydroxytamoxifen (4-OHT). To inhibit RNA polymerase II transcription or SPHK1 activity cells were treated with 1 μM flavopiridol for 1–3 h or 10 μM of SKI II, respectively. To monitor RNA half-life, U2OS/ER-E2F1 cells were induced with 200 nM 4-OHT at 60% confluency for 5 h. After addition of 1 μM flavopiridol, cells were harvested in 20 min intervals, RNA was isolated and quantified by RT-qPCR.

### Recombinant plasmids preparation

pTet-*KHPS1*/+1448/-592 comprises *SPHK1* sequences from –592 to +1448 with respect to the TSS of *SPHK1-B* inserted into pTet-7B-MS2bs. To generate reporter constructs containing foreign TFR sequences, oligonucleotides comprising TFR sequences were annealed and inserted between the BamHI and *Csil* sites of pTet-*KHPS1*/+1448/-592. Oligonucleotide sequences are listed in Table S4. To generate pREP4-luc, the luciferase gene from pGL4.10 was inserted into the *NheI*-*BamHI* site of the episomal vector pREP4. Luciferase reporter constructs were cloned by inserting PCR fragments comprising *SPHK1* sequences –592/+1795, +46/+1795 or –592/+1795Δ(+706/+1189) into pREP4-luc. To generate pTet-*KHPS1*(+1448/-592)isoB-luc, a PCR fragment comprising nucleotides –592/+1448 was inserted into pTet-7B-MS2bs-luc. To produce pTet-7B-MS2bs-luc, the luciferase gene from pGL4.10 was cloned into the *XhoI* site of pTet-7B-MS2bs. Primer sequences are listed in Table S3.

### RNA isolation and quantitative RT-PCR

RNA was isolated using TRI reagent. For reverse transcription, RNA was treated with TURBO DNase I and transcribed into cDNA with Transcriptor Reverse Transcriptase using 2 μg of RNA and 0.25 μM of random hexamer primers. qPCR was performed on a Roche LightCycler 480 using the QuantiTect SYBR Green PCR Kit and gene-specific primers. RNA levels were normalized to 18S rRNA. To analyze antisense and sense transcripts from the reporter plasmid pTet-*KHPS1*(+1448/-592) or pREP4-*SPHK1*(–592/+1795)-luc, cDNA was synthesized by strand-specific RT using primers +841R and –89F, respectively. Primers are listed in Table S3.

Synthetic RNAs were generated by *in vitro* transcription using MEGAscript T7 Transcription Kit (Ambion) according to the manufacturer's instructions. To label RNA, the reaction mixture was supplemented with 2.5 nM biotin-16-dUTP (Roche). Templates were generated by PCR using gene specific reverse primers fused to T7 promoter sequence (Table S3).

### Luciferase assay

U2OS/ER-E2F1 or NIH 3T3 TetON cells seeded in 12 well plates were transfected with 50 ng of the respective firefly luciferase reporter plasmids and 5 ng of the TK-*Renilla* plasmid (Promega). Cells were lysed in 1x Passive Lysis Buffer (Promega) 24 h after transfection, and luciferase activity was measured by monitoring light emission with the *in vivo* imaging system of IVIS Lumina II instrument (PerkinElmer). Firefly luciferase activity was normalized to *Renilla* luciferase activity and presented in reference to expression of the control reporter vector.

### Chromatin immunoprecipitation (ChIP)

Cells were crosslinked with 1% formaldehyde for 10 min, quenched with 125 mM glycine. Isolated chromatin was sonicated in a Bioruptor Pico (Diagenode) in buffer containing 1% SDS, 50 mM HEPES [pH 8.0], 10 mM EDTA to obtain an average fragment length of 200–500 bp. For ChIPs on reporter plasmids, the chromatin pellets were digested with a cocktail of restriction enzymes (*XhoI*, *Scal*, *BspEI*, *SapI*) prior to sonication. Upon dilution with 4 volumes of IP-buffer (20 mM HEPES [pH 8.0], 187.5 mM NaCl, 1 mM EDTA, 0.5 mM EGTA, 1% Triton X-100), chromatin was incubated with antibody-coupled Dynabeads coated with Protein G overnight at 4°C. Protein-DNA complexes were washed twice in buffer A (150 mM NaCl, 20 mM HEPES [pH 8.0], 0.5 mM EGTA, 1 mM EDTA,

0.1% SDS, 0.1% Na-deoxycholate, 1% Triton X-100), followed by two washes with buffer B containing 500 mM NaCl, with buffer C (250 mM LiCl, 0.5% Na-deoxycholate, 0.5% NP-40, 20 mM HEPES [pH 8.0], 0.5 mM EGTA, 1 mM EDTA), and with buffer D (20 mM HEPES [pH 8.0], 0.5 mM EGTA, 1 mM EDTA). After elution, reversal of the cross-link (65°C, 6 h) and digestion with proteinase K, DNA was purified and quantified by qPCR using gene-specific primers. Primer sequences are listed in Table S3. The ratio of DNA in the immunoprecipitates (upon subtraction of the IgG background) versus DNA in the input chromatin was calculated and normalized to control reactions.

### RNA immunoprecipitation (RIP)

Nuclei were lysed in RIP buffer (20 mM Tris-HCl [pH 8.0], 200 mM NaCl, 1 mM EDTA, 1 mM EGTA, 0.5% Triton X-100, 1% NP-40, 100 U RNasin, and Roche Complete protease inhibitors) for 15 min at 4°C. After brief sonication and treatment with DNase I, lysates were sonicated, cleared by centrifugation, diluted 5-fold in RIP buffer without detergents and incubated with the respective antibodies coupled to Dynabeads Protein G for 3.5 h at 4°C. Immobilized protein-RNA complexes were washed 3 times in buffer containing 400 mM NaCl, 20 mM Tris-HCl [pH 8.0], 1 mM EDTA, 1 mM EGTA, 100 U RNasin, protease inhibitors (Roche Complete), 0.2% NP-40, 0.1% Triton X-100. Co-precipitated RNA was eluted for 30 min at 56°C in buffer containing 20 mM Tris-HCl [pH 8.0], 30 mM NaCl, 2.5 mM EDTA, 0.4% SDS, 20 mg/ml proteinase K, purified with TRIzol and analyzed by RT-qPCR. The fraction of co-precipitated RNA is calculated as percentage of input normalized to the IgG signal and presented in the reference to the control reaction.

### Cross-linking and immunoprecipitation (CLIP) assay

U2OS/ER-E2F1 cells were crosslinked with 150 mJ/cm<sup>2</sup> at 254 nm using a Stratelinker (Stratagene). Nuclei were isolated and lysed in RIPA buffer (10 mM Tris-HCl [pH 7.5], 140 mM NaCl, 1% Triton X-100, 0.1% Na-deoxycholate, 100 U RNasin, and protease inhibitors). RNA was digested for 3 min with 0.1 U RNase I and 4 U TURBO DNase. After clearing by centrifugation, the lysates were diluted 1:3 with RIPA buffer without SDS and incubated with antibody-coupled Protein G Dynabeads overnight at 4°C. After stringent washing in 50 mM Tris-HCl [pH 7.5], 1 M NaCl, 1 mM EDTA, 1% NP-40, 0.1% SDS, 0.5% Na-deoxycholate, co-precipitated RNA was eluted by incubation at 37°C for 30 min in buffer containing 0.5% SDS and 200 ng/ml proteinase K and for another 30 min with the same buffer containing 7 M urea. RNA was analyzed by RT-qPCR, the fraction of co-precipitated *KHPS1* being presented as percentage of input normalized to the IgG signal.

### Triplex Capture Assay

100 fmoles of PCR-fragments containing *eSPHK1* sequence from -406 to -65 were digested with exonuclease I and incubated with 1 pmol of biotin-labeled *KHPS1* (-373/-241) in 10 mM Tris-HCl [pH 7.5], 20 mM KCl, 10 mM MgCl<sub>2</sub>, 0.05% Tween 20, and 100 U of RNasin (Promega) for 1.5 h at room temperature. RNA-DNA complexes were captured on Dynabeads MyOne Streptavidin C1 beads, washed three times with a buffer containing 150 mM KCl, 10 mM Tris-HCl [pH 7.5], 5 mM MgCl<sub>2</sub>, 0.5% NP-40, and once with buffer containing 15 mM KCl, 10 mM Tris-HCl [pH 7.5] and 5 mM MgCl<sub>2</sub>. RNA-associated DNA was eluted with RNase A (50 ng/ml, 30 min at 37°C), analyzed by qPCR, normalized to input DNA and presented in reference to control sample. To monitor recovery of *eSPHK1* sequences, primers -406/-304 were used. To generate 7-deaza-modified DNA fragments, 7-deaza-2-deoxy-nucleotide-5'-triphosphate (7-deaza-dGTP) and 7-deaza-2-deoxy-adenosine-5'-triphosphate (7-deaza-dATP) and the PwoSuperYield DNA polymerase Kit were used in PCR reactions.

### Wound-healing and invasion assays

To monitor cell migration, a wound healing assay was performed in MDA-MB-231 cells transfected with ASOs or synthetic RNAs. Confluent cells were wounded by manual scratching with a 10  $\mu$ L pipette tip. Plates were photographed immediately and 24 h after scratching using Nikon microscope (Eclipse TE2000). For Matrigel invasion assay,  $5 \times 10^4$  cells were suspended in 0.3 mL medium containing 10% serum, plated in the top chamber with a Matrigel-coated membrane (24-well insert; pore size, 8  $\mu$ m, (Corning Biocat) with 0.5 mL medium containing 20% serum as an attractant at the lower chamber. 16 h after seeding, cells in lower part of the chamber were fixed with 100% methanol and stained with 0.5% crystal violet.

### Soft agar colony formation assay

$5 \times 10^3$  MDA-MB-231 cells in medium containing 0.2% agarose were plated on top of a bottom layer containing 0.5% agarose and 20% serum. After incubation for 20-30 days with medium changes every three days, colonies were stained with 0.5% crystal violet and images were taken.

## QUANTIFICATION AND STATISTICAL ANALYSIS

All experiments were performed in the form of matched pairs in which “control” and “experimental” samples were paired. The values in the graphs show means of three independent experiments with error bars representing standard error of the mean (SEM). The statistical significance level was set at p values \*p < 0.05, \*\*p < 0.01 and \*\*\*p < 0.001 calculated using a paired two-tailed Student's t test with two groups of unnormalized data.